2021 43rd Annual International Conference of the
IEEE Engineering in Medicine & Biology Society (EMBC)
Oct 31 - Nov 4, 2021. Virtual Conference

Personal Identification Using Gait Spectrograms and Deep Convolutional Neural Networks

Dawoon Jung, Mau Dung Nguyen, Muhammad Zeeshan Arshad, Jinwook Kim, and Kyung-Ryoul Mun

Abstract—**Human gait can serve as a useful behavioral trait for biometrics. Compared to fingerprint, face, and iris, the most commonly used physiological identifiers, gait can be unobtrusively monitored from a distance without requiring explicit involvement and physical restraint from people. Advances in wearable technology facilitate direct and faithful measurement of gait motions with easy-to-use and low-cost inertial sensors. This study aimed to propose an approach to using kinematic gait data collected with wearable inertial sensors for reliable personal identification. Sixty-nine individuals ranged in age from 24 to 62 years old participated in this study. The 3-axis acceleration and the 3-axis angular velocity signals were measured using the inertial measurement units attached to the feet, shanks, thighs, and posterior pelvis while walking. The gait spectrograms were acquired by applying time-frequency analyses to the lower body movement signals measured in one stride. Among each participant's 15 strides, 12 strides were used in the 4-fold cross validation of the deep convolutional neural network-based classifiers, and the remaining three strides were used to evaluate the classifiers. An accuracy of 99.69% was achieved by using the foot, shank, thigh, and pelvic spectrograms, and the accuracy was 96.89% using only the foot spectrograms. This study has the potential to be applied in behavior-based biometric technologies by confirming the feasibility of the proposed kinematic and spectrographic approaches in identifying personal behavioral characteristics.**

Clinical Relevance—**The proposed approach for automatic and effective personal identification can be utilized in smart residential and care facilities to provide customized healthcare services through unobtrusive gait monitoring of individuals.**

I. Introduction

Intelligent robots and systems in smart environments can play a very important role in improving quality of life of human beings based on ambient intelligence (AmI). Especially, residential and care facilities with cloud computing and Internet of Things environments can provide customized life-enriching services through unobtrusive long-term monitoring of individuals using wearable and ambient devices or mobile robots. As an indispensable technology to realize the foregoing, biometrics has been drawing attention for automatic and effective personal recognition and identification.

Biometric identifiers are categorized into physiological identifiers and behavioral identifiers. Fingerprint, palm, face, iris, and vein pattern are included in the physiological identifiers. The behavioral identifiers include voice, signature, gestures, keyboard typing pattern, and other traits that can be extracted from user actions. Human gait, defined as a personal manner of walking, is also a behavioral identifier because it is determined by an individual's intrinsic factors (e.g., sex, age, etc.), physical factors (e.g., weight, height, limb length, physique, etc.), psychological factors (e.g., personality type, etc.), and pathological factors (e.g., musculoskeletal anomalies, neurological diseases, psychiatric disorders, etc.) [1]. The most popular biometric identifiers are fingerprint, face, and iris, which require close access to the scanners and active cooperation from the users during the recognition procedure. Whereas gait can be unobtrusively monitored from a distance without requiring explicit involvement and physical restraint from the users. Hence gait has been strongly supported as a useful biometric identifier [2, 3].

Most researches on gait-based personal identification were performed by recognizing human gait in images or videos recorded with cameras [2, 4-11]. However, the vision-based gait recognition was challenged by imperfect foreground segmentation of the walker from the background scene, variations in the camera viewing angle, alterations in clothing and in carrying condition of the walker, changes in illumination, ambient occlusion, clutter, and other perceptual distortions [5, 12]. Also, using camera equipment signifies the vision-based approach is only suitable for fixed locations. With the recent development of microelectromechanical systems, collecting kinematic data of body movements using inertial sensors has become widely applied in gait studies owing to many positive features of inertial sensors such as small size, light in weight, portability, easiness to use, low cost, and low power consumption. Our previous study, which achieved multiple classification of gait by analyzing the lower body six-degree-of-freedom (6-DOF) motions measured with wearable inertial measurement units (IMUs), suggested promising potential of kinematic gait data as reliable biometric identifiers [1]. Several previous studies, which developed ambulatory gait monitoring systems using inertial sensors embedded in footwear or accessory and using a smartphone, suggested promising real-world applicability of kinematic gait data as practical biometric identifiers [13, 14].

The aim of this study was to propose an approach to using kinematic gait data collected with wearable IMUs for reliable personal identification. To achieve this aim, a time-frequency

*Research supported by the Korea Institute of Science and Technology (KIST) Institutional Program (Project No. 2E31051) and the Korea Medical Device Development Fund grant funded by the Korea government (the Ministry of Science and ICT, the Ministry of Trade, Industry and Energy, the Ministry of Health & Welfare, the Ministry of Food and Drug Safety) (Project No. 1711139131).

D. Jung, M. D. Nguyen, M. Z. Arshad, J. Kim, and K. Mun are with the Center for Artificial Intelligence, KIST, Seoul, Republic of Korea (corresponding author to provide phone: +82-2958-6785; fax: +82-2958-5769; e-mail: krmoon02@kist.re.kr).

analysis was employed for effective representation of kinematic gait data. The gait representations were used to train the deep convolutional neural network (DCNN)-based classifiers. This study is expected to be utilized for unobtrusive personal identification in AmI environments. By confirming the feasibility of the proposed analytic approach in identifying personal behavioral characteristics, this study can give inspiration not only to gait-based biometrics but also to other behavior-based biometric technologies.

II. Materials and Methods

A. Participants

A total of 69 individuals able to ambulate at least 20 meters without any walking aids or assistance from other people participated in this study. The participants ranged in age from 24 to 62 years with the mean of 38.77 years. The height and weight (mean ± SD) of the participants were 173.27 ± 6.10 cm and 70.91 ± 7.76 kg, respectively. All participants provided written informed consent before their participation. This study was approved by the Institutional Review Board of Korea Institute of Science and Technology.

B. Experimental protocol

The 3-axis acceleration and the 3-axis angular velocity signals were measured using seven commercialized wearable IMUs (Xsens MVN, Enschede, Overijssel, Netherland) at a sampling frequency of 100 Hz. Each IMU was 47 mm long, 30 mm wide, and 13 mm height with a weight of 16 g. Fig. 1(a) shows the *x*-, *y*-, and *z*-axis of the IMU, and Fig. 1(b) depicts the locations of the IMUs: on both feet (middle of the bridge of foot), on both shanks (medial surface of the tibia), on both thighs (the lateral side above the knee), and on posterior pelvis (flat on the sacrum) [1, 15]. Each participant was instructed to walk three times, each at slow, preferred, and fast speeds, on the 20-meter straight and flat path. The participants were requested to walk 15% to 25% slower and faster than their preferred speed for their slow and fast speeds.

C. Gait assessment

Gait cycle detection

The measured acceleration and angular velocity signals were band-pass filtered between 0.1 and 15 Hz and then upsampled to 1000 Hz using spline interpolation. These signals were normalized for data scaling into the range [-1, 1] to minimize the effect of proximal-distal displacement of IMUs. Using the heel-strike (HS) and toe-off (TO) times of both lower limbs acquired from the angular velocity signals measured at both feet and both shanks, the following gait parameters were calculated: stance time (time elapsed from a HS to a TO of the same foot), swing time (time elapsed from a TO to a HS of the same foot), double limb support (DLS) time (amount of time spent with both feet contacting the ground), single limb support (SLS) time (amount of time spent with only one foot contacting the ground), step time (time elapsed between a HS and a consecutive HS of the opposite foot), stride time (time elapsed between a HS and a consecutive HS of the same foot), step length (distance between a HS and a consecutive HS of the opposite foot), stride length (distance between a HS and a consecutive HS of the same foot), and gait velocity (value calculated by dividing a stride length into a corresponding stride time) [16-19]. The stride and step lengths were normalized with the height of each participant. Each participant's five strides observed in the middle of the walkway were extracted for each of the slow-, preferred-, and fast-speed walking trials. The acceleration and angular velocity signals measured in each stride at the both feet, both shanks, both thighs, and posterior pelvis were used in the analysis.

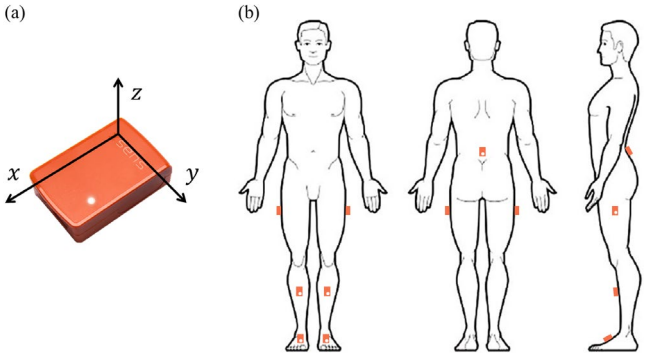

Figure 1. (a) Three axes of the inertial measurement unit (IMU) and (b) seven locations of the IMUs.

Gait representation

Continuous wavelet transform (CWT) was employed to represent the lower body movements with information on frequency and power that vary with time. CWT is defined as follows:

$$\mathrm{CWT}\{x(t)\} = X(a,b) = \frac{1}{\sqrt{a}}\int_{-\infty}^{\infty} x(t)\psi^*\left(\frac{t-b}{a}\right)e^{-j\omega t}dt \quad (1)$$

where $x(t)$ and $\psi(t)$ denote signals to be transformed and a mother wavelet, such as Morlet, Daubechies, and Meyer wavelets, respectively. a, b, and * indicate scale of wavelet transform, time shift, and complex conjugation, respectively [20]. The magnitude squared of CWT yields a spectrogram of the following function:

$$\mathrm{spectrogram}\{x(t)\} = |X(a,b)|^2 \quad (2)$$

In this study, each of the acceleration and angular velocity signals was multiplied by the Morlet wavelet, and the magnitude squared of the transformed signals was regarded as a gait spectrogram. Fig. 2(a) shows the *y*-axis foot acceleration signals measured in a preferred-speed stride of one participant [15]. Fig. 2(b) displays the spectrogram obtained by applying CWT to the signals in Fig. 2(a). The orange and yellow areas in Fig. 2(b) denote higher energies of the specific frequency components compared to other components [15].

By depicting the lower body movements in 15 strides of each of the 69 participants with 3-axis acceleration and 3-axis angular velocity signals measured at seven locations, a total of 43,470 spectrograms were acquired.

Statistical analysis

One-way analysis of variance (ANOVA) was performed using SPSS statistics software (v.25.0, SPSS Inc., Chicago, Illinois, USA) to investigate the significance of differences in gait parameter values depending on walking speed.

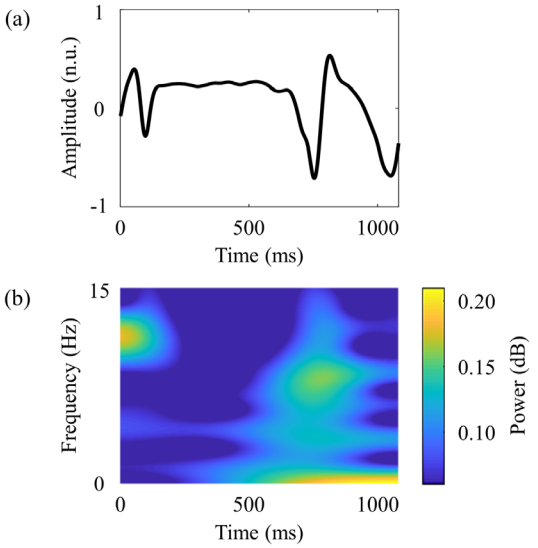

Figure 2. (a) Acceleration signals in *y*-axis measured at the foot in a preferred-speed stride and (b) a spectrogram obtained by applying continuous wavelet transform to the signals in (a).

D. Classifier training and evaluation

Each input image set of the DCNN-based classifiers was designated as SP_X, which denoted the set of spectrograms obtained from the signals measured at X that was feet (F), shanks (S), thighs (T), posterior pelvis (P), feet and posterior pelvis (FP), or feet, shanks, thighs, and posterior pelvis (FSTP). The spectrogram set of each lower body segment was produced according to the following steps. First, each of the six spectrograms of the 3-axis acceleration signals and the 3-axis angular velocity signals was resized to 768 × 384 × 3 (3-channel RGB image). Second, the resized spectrogram of *x*-axis acceleration signals was piled upon that of *x*-axis angular velocity signals, which provided the new image with a size of 768 × 768 × 3. By applying the second step to each spectrogram of *y*- and *z*-axis signals, two more new images each with a size of 768 × 768 × 3 were obtained. Third, three new images were stacked back in the order of *x*-, *y*-, and *z*-axis. These steps were used to produce the left foot, the right foot, the left shank, the right shank, the left thigh, the right thigh, and the pelvic spectrogram sets each with a size of 768 × 768 × 9. Whereas the size of SP_P was identical with the size of the pelvic spectrogram set, the sizes of SP_F, SP_S, and SP_T were 768 × 768 × 18 because each of them was acquired by stacking the right side spectrogram set behind the left side spectrogram set. The combination of SP_F and SP_P corresponded to SP_{FP} with a size of 768 × 768 × 27. Fig. 3 depicts SP_{FSTP} with a size of 768 × 768 × 63, which was obtained by stacking SP_F, SP_S, SP_T, and SP_P.

Each of the ResNet18-, ResNet50-, and DenseNet121-based classifiers was used for the personal identification. The classifiers were trained using adaptive moment estimation (Adam) optimizer with a batch size of 16 and a learning rate of 0.0001. A dropout probability of 0.6 was applied in the last layer. Regarding the learning rate schedule, the learning rate was reduced on a plateau of validation set accuracy with a factor of 0.5 and a patience of two epochs. The training process was early stopped when the accuracy for the validation set was not improved within seven epochs. Among each participant's 15 strides, 12 strides were used in the 4-fold cross validation of the classifiers, and the remaining three strides were used to evaluate the classifiers. The personal identification performance was multi-evaluated with consideration for the three different classifiers and the six different input image sets.

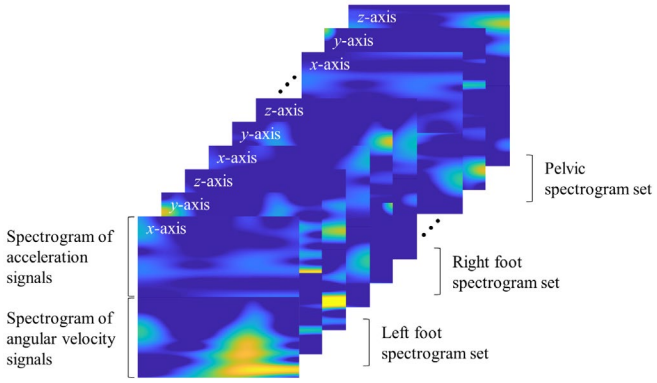

Figure 3. Configuration of the spectrograms to use as an input image set of deep convolutional neural network models.

III. Results

A. Gait parameters

Table I summarizes the gait parameter values of all participants depending on walking speed. The mean and SD values of the gait velocities were 1.09 ± 0.22 m/s, 1.43 ± 0.18 m/s, and 1.81 ± 0.25 m/s in the slow-, the preferred-, and the fast-speed walking trials, respectively, and the one-way ANOVA with Dunnett's T3 post-hoc test revealed the significant differences among these values ($P < 0.001$). The significance of differences in the other gait parameters depending on walking speed were observed from the one-way ANOVA with Tukey's post-hoc test (equal variance) or with Dunnett's T3 post-hoc test (unequal variance) (all $P < 0.05$).

B. Identification performance

Fig. 4(a) and 4(b) show the top-1 and the top-3 accuracies, respectively, resulted by using SP_F, SP_S, SP_T, or SP_P as an input image set of the three classifiers for the personal

TABLE I. Gait Parameters of The Study Participants

Gait parameter	Walking speed		
	Slow	***Preferred***	***Fast***
Gait velocity (m/s)	1.09 ± 0.22	1.43 ± 0.18*	1.81 ± 0.25*†
Stance time (s)	0.79 ± 0.16	0.65 ± 0.10*	0.57 ± 0.07*†
Swing time (s)	0.60 ± 0.11	0.52 ± 0.09*	0.49 ± 0.07*†
DLS[a] time (s)	0.11 ± 0.05	0.08 ± 0.04*	0.06 ± 0.04*†
SLS[b] time (s)	0.60 ± 0.11	0.52 ± 0.08*	0.49 ± 0.07*†
Step time (s)	0.70 ± 0.13	0.59 ± 0.09*	0.53 ± 0.07*†
Stride time (s)	1.39 ± 0.25	1.17 ± 0.17*	1.05 ± 0.13*†
Step length (m)	0.39 ± 0.05	0.44 ± 0.04*	0.50 ± 0.05*†
Stride length (m)	0.78 ± 0.08	0.87 ± 0.07*	0.99 ± 0.09*†

a. Double limb support; b. Single limb support.

Data are presented as the mean ± SD.

*$P < 0.05$ in comparison to the slow speed; †$P < 0.05$ in comparison to the preferred speed.

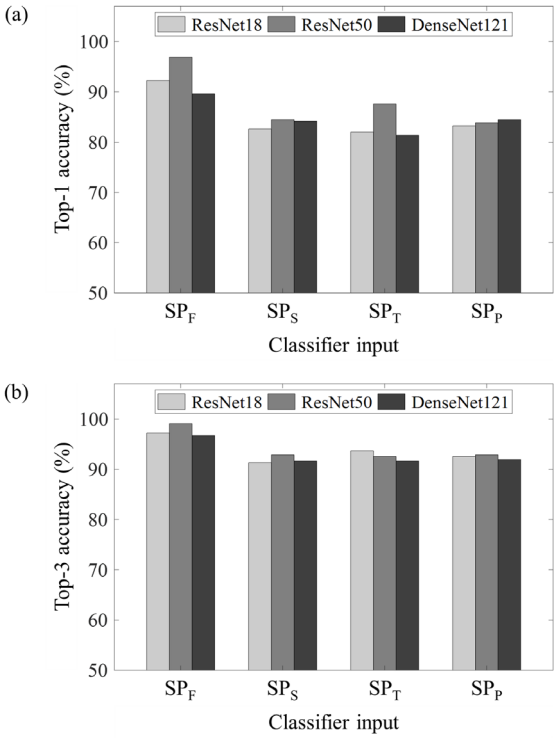

Figure 4. (a) Top-1 accuracies and (b) top-3 accuracies in the personal identification using the three different deep convolutional neural network-based classifiers trained with the foot spectrograms (SP_F), the shank spectrograms (SP_S), the thigh spectrograms (SP_T), or the pelvic spectrograms (SP_P).

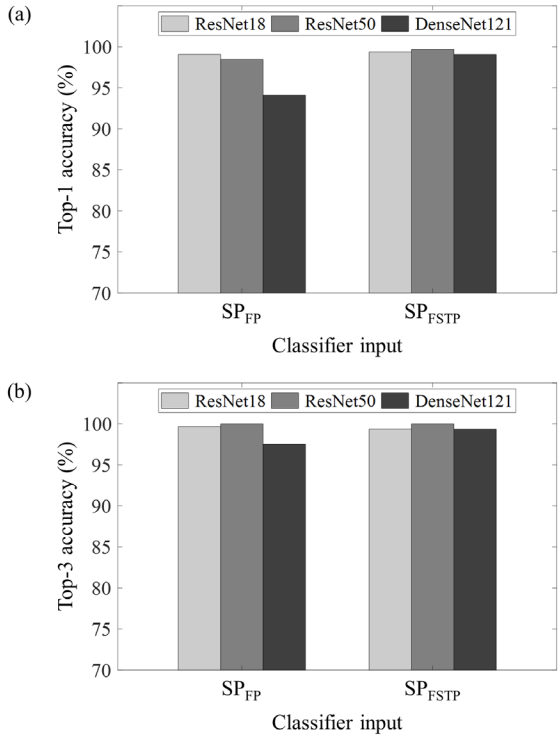

Figure 5. (a) Top-1 accuracies and (b) top-3 accuracies in the personal identification using the three different deep convolutional neural network-based classifiers trained with the foot and pelvic spectrograms (SP_{FP}) or the foot, shank, thigh, and pelvic spectrograms (SP_{FSTP}).

identification. The highest value among the top-1 accuracies in Fig. 4(a) was 96.89%, and that among the top-3 accuracies in Fig. 4(b) was 99.07%. Both of these values were obtained from the ResNet50-based classifier trained with SP_F.

The top-1 and the top-3 accuracies, the results of using SP_{FP} or SP_{FSTP} as an input image set of the three classifiers, were displayed in Fig. 5(a) and 5(b), respectively. The greatest top-1 accuracy in the personal identification using SP_{FP} was 99.07% obtained by the ResNet18-based classifier. The use of SP_{FSTP} resulted in top-1 accuracies of 99.38% for the ResNet18-based classifier, 99.69% for the ResNet50-based classifier, and 99.07% for the DenseNet121-based classifier. Top-3 accuracies of 100% were provided from the ResNet50-based classifiers trained with SP_{FP} or SP_{FSTP}.

Table II summaries the personal identification performance of each input image set with the mean and SD values of the top-1 and the top-3 accuracies resulted by using the three different classifiers.

IV. Discussion

This study proposed the approach to using gait spectrograms and DCNNs for reliable personal identification. The spectrographic analysis on the three translations and the three rotations of each lower body segment in one stride was effective to represent kinematic features of gait. The foot, shank, thigh, and pelvic spectrograms trained with the ResNet50-based classifier exhibited the outstanding performance, 99.69% accuracy, in identifying the 69 individuals regardless of walking speed. Johnston *et al*. obtained up to 79.2% accuracy in the gait-based personal identification using the time-series features of the acceleration and the angular velocity signals measured for 10 seconds with a smartwatch from the 36 subjects [21]. Derawi *et al*. recognized gait by applying a cross dynamic time warping metric to the acceleration data collected with a smartphone while walking 30 meters and identified the 25 subjects with 89.3% accuracy [22]. By extracting six time-series features from the accelerometer data collected with a cell phone in one's pocket during 10-second walking, Kwapisz *et al*. acquired a personal identification accuracy of 90.9% for the 36 subjects [23]. Pan *et al*. recognized the gait pattern with the signature points extracted from the acceleration signals measured for 10 seconds using the accelerometers attached to the wrist, upper arm, waist, thigh, and ankle. They achieved up to 96.7% identification accuracy for the 30 subjects [24]. Compared to the abovementioned studies, this study achieved

TABLE II. Personal Identification Performance

Classifier input	Top-1 accuracy (%)	Top-3 accuracy (%)
SP_F[a]	92.91 ± 3.69	97.67 ± 1.24
SP_S[b]	83.75 ± 1.00	91.92 ± 0.82
SP_T[c]	83.65 ± 3.42	92.60 ± 1.01
SP_P[d]	83.85 ± 0.62	92.45 ± 0.47
SP_{FP}[e]	97.21 ± 2.71	99.07 ± 1.35
SP_{FSTP}[f]	99.38 ± 0.31	99.59 ± 0.36

a. Foot spectrograms; b. Shank spectrograms; c. Thigh spectrograms; d. Pelvic spectrograms; e. Foot and pelvic spectrograms; f. Foot, shank, thigh, and pelvic spectrograms.

Data are presented as the mean ± SD.

more accurate identification for more individuals with less cumbersome feature extraction process. In other words, representing the kinematic gait data as spectrograms was helpful to reduce a lot of manual labor, time-consuming and resource-intensive processes, and empirical knowledge for feature engineering. It is also noteworthy that this study only used the information on one stride observed for about one second in a space of about one-meter long.

As shown in Fig. 4, using the foot spectrograms was more effective than using the shank, the thigh, or the pelvic spectrograms in the personal identification. This result would be related to the anatomical structure of the lower body. As the most distal part of the lower body, the foot is the part where 6-DOF motions at the ankle, dorsi-/plantar-flexion, abduction/adduction, and inversion/eversion, can be faithfully observed [25]. Therefore, the various gait characteristics could be included in the foot movements, and thus the foot spectrogram set could be an effective personal identifier. By combining the foot spectrograms with the pelvic spectrograms, the identification performance was improved because the pelvic movements could also contain various gait characteristics related to the pelvic rotation, obliquity, and tilt which were known as primary determinants of human locomotion [26]. On the other hand, the shank movements were affected by the knee motions with constraints on abduction/adduction and internal/external rotation in the gait cycle. This restriction was also observed in the hip motion, which affected the thigh movements, during walking [25]. Hence the shank and the thigh spectrograms would have limitations in exhibiting various gait characteristics and consequently were less effective as personal identifiers. With gait involving chain activities of the different lower body segments, using the foot, shank, thigh, and pelvic spectrograms altogether could provide the best performance in the personal identification.

In terms of real-world applicability and usability, it is notable that the proposed approach achieved up to 96.89% accuracy in personal identification only with the foot spectrograms obtained in one stride regardless of walking speed. The performance of the foot and pelvic spectrograms reported as an accuracy of up to 99.07% is also noteworthy. A promising user acceptance of the proposed approach can be expected because foot and pelvic movements can be readily and easily monitored with wearable sensors such as footwear- and belt-attached IMUs. The high user acceptance of a foot bracelet sensor and that of a lower back sensor were verified by Giansanti *et al*. and by Zhong *et al*., respectively [27, 28]. Hence the proposed approach has the potential to be utilized in smart residential and care facilities for providing customized AmI services to each occupant. This study is expected to give inspiration not only to gait-based biometrics but also to other behavior-based biometric technologies by confirming the feasibility of the proposed analytic approach in identifying personal behavioral characteristics.

This study has some limitations related to generalizability. Applying the proposed approach to larger groups with diverse demographic, anthropometric, and pathological characteristics needs to be carried out along with lower body movement signal acquisition using readily available devices such as an accelerometer- and gyroscope-equipped smartphone. Confirming within-day and day-to-day reproducibility of the proposed approach is also required. Further studies will be conducted for improving the proposed approach to be less sensitive to inertial sensor orientation by calibrating the acceleration and angular velocity signals. Feasibility of biometric authentication using the gait spectrograms will be assessed in future work to extend the utilization of this study in secure systems and forensic science.

V. Conclusion

This study proposed the approach that enabled reliable personal identification using the gait spectrograms and DCNNs. The 3-axis acceleration and the 3-axis angular velocity signals measured at the feet, shanks, thighs, and posterior pelvis in one stride were represented as gait spectrograms. The DCNN models trained with the gait spectrograms exhibited outstanding performance in identifying the individuals regardless of walking speed. This study pioneered the utilization of kinematic and spectrographic approaches to identify personal behavioral characteristics, which has great potential to improve behavior-based biometric technologies.

Acknowledgment

This research was supported by the Korea Institute of Science and Technology Institutional Program (Project No. 2E31051) and the Korea Medical Device Development Fund grant funded by the Korea government (the Ministry of Science and ICT, the Ministry of Trade, Industry and Energy, the Ministry of Health & Welfare, the Ministry of Food and Drug Safety) (Project No. 1711139131).

References

[1] D. Jung *et al*., "Deep neural network-based gait classification using wearable inertial sensor data," in *IEEE Int. Engineering in Medicine and Biology Conf*., 2019, pp. 3624-3628.

[2] L. Wang, T. Tan, H. Ning, and W. Hu, "Silhouette analysis-based gait recognition for human identification," *IEEE Trans. Pattern Anal. Mach. Intell.,* vol. 25, no. 12, pp. 1505-1518, 2003.

[3] C. Zhang, W. Liu, H. Ma, and H. Fu, "Siamese neural network based gait recognition for human identification," presented at the IEEE Int. Conf. on Acoustics, Speech, and Signal Processing, 2016.

[4] J. Little and J. Boyd, "Recognizing people by their gait: the shape of motion," *Videre: Journal of Computer Vision Research,* vol. 1, no. 2, pp. 1-32, 1998.

[5] L. Lee and W. E. L. Grimson, "Gait analysis for recognition and classification," in *IEEE Int. Conf. on Automatic Face Gesture Recognition*, 2002, pp. 155-162.

[6] M. Hu and Y. Wang, "A new approach for gender classification based on gait analysis," in *IEEE Int. Conf. on Image and Graphics*, 2009, pp. 869-874.

[7] Y. Makihara, H. Mannami, and Y. Yagi, "Gait analysis of gender and age using a large-scale multi-view gait database," in *Asian Conf. on Computer Vision*, 2010, pp. 440-451.

[8] M. Hu, Y. Wang, Z. Zhang, and D. Zhang, "Gait-based gender classification using mixed conditional random field," *IEEE Trans. Syst., Man, Cybern. B. Cybern.,* vol. 41, no. 5, pp. 1429-1439, 2011.

[9] M. Deng, C. Wang, and T. Zheng, "Individual identification using a gait dynamics graph," *Pattern Recognit.,* vol. 83, pp. 287-298, 2018.

[10] O. M. S. Hassan, A. M. Abdulazeez, and V. M. TİRYAKİ, "Gait-based human gender classification using lifting 5/3 wavelet and principal component analysis," in *IEEE Int. Conf. on Advanced Science and Engineering*, 2018, pp. 173-178.

[11] M. Babaee, L. Li, and G. Rigoll, "Person identification from partial gait cycle using fully convolutional neural networks," *Neurocomputing,* vol. 338, pp. 116-125, 2019.
[12] A. Mannini, D. Trojaniello, A. Cereatti, and A. M. Sabatini, "A machine learning framework for gait classification using inertial sensors: Application to elderly, post-stroke and huntington's disease patients," *Sensors,* vol. 16, no. 1, p. 134, 2016.
[13] F. Lin, A. Wang, Y. Zhuang, M. R. Tomita, and W. Xu, "Smart insole: A wearable sensor device for unobtrusive gait monitoring in daily life," *IEEE Trans. Industr. Inform.,* vol. 12, no. 6, pp. 2281-2291, 2016.
[14] R. LeMoyne and T. Mastroianni, "Wearable and wireless gait analysis platforms: smartphones and portable media devices," in *Wireless MEMS Networks and Applications*: Elsevier, 2017, pp. 129-152.
[15] D. Jung, M. D. Nguyen, M. Park, J. Kim, and K.-R. Mun, "Multiple classification of gait using time-frequency representations and deep convolutional neural networks," *IEEE Trans. Neural Syst. Rehabil. Eng.,* vol. 28, no. 4, pp. 997-1005, 2020.
[16] K. Aminian, B. Najafi, C. Büla, P. F. Leyvraz, and P. Robert, "Spatio-temporal parameters of gait measured by an ambulatory system using miniature gyroscopes," *J. Biomech.,* vol. 35, no. 5, pp. 689-699, 2002.
[17] J. H. Hollman, E. M. McDade, and R. C. Petersen, "Normative spatiotemporal gait parameters in older adults," *Gait Posture,* vol. 34, no. 1, pp. 111-118, 2011.
[18] J. Kamruzzaman and R. K. Begg, "Support vector machines and other pattern recognition approaches to the diagnosis of cerebral palsy gait," *IEEE Trans. Biomed. Eng.,* vol. 53, no. 12, pp. 2479-2490, 2006.
[19] K. R. Mun, G. Song, S. Chun, and J. Kim, "Gait estimation from anatomical foot parameters measured by a foot feature measurement system using a deep neural network model," *Sci. Rep.,* vol. 8, no. 1, pp. 1-10, 2018.
[20] S. Mallat, *A wavelet tour of signal processing: The sparse way*, 3rd ed. Elsevier, 2009.
[21] A. H. Johnston and G. M. Weiss, "Smartwatch-based biometric gait recognition," in *IEEE Int. Conf. on Biometrics Theory, Applications and Systems*, 2015, pp. 1-6.
[22] M. Derawi and P. Bours, "Gait and activity recognition using commercial phones," *Comput. secur.,* vol. 39, pp. 137-144, 2013.
[23] J. R. Kwapisz, G. M. Weiss, and S. A. Moore, "Cell phone-based biometric identification," in *IEEE Int. Conf. on Biometrics: Theory, Applications and Systems*, 2010, pp. 1-7.
[24] G. Pan, Y. Zhang, and Z. Wu, "Accelerometer-based gait recognition via voting by signature points," *Electron. Lett.,* vol. 45, no. 22, pp. 1116-1118, 2009.
[25] S. Giannini, F. Catani, and M. G. Benedetti, *Gait analysis: methodologies and clinical applications*. IOS press, 1994.
[26] V. T. Inman and H. D. Eberhart, "The major determinants in normal and pathological gait," *J. Bone Jt. Surg.,* vol. 35, no. 3, pp. 543-558, 1953.
[27] R. Zhong, P. L. P. Rau, and X. Yan, "Gait assessment of younger and older adults with portable motion-sensing methods: A user study," *Mob. Inf. Syst.,* pp. 1-13, 2019.
[28] D. Giansanti, S. Morelli, G. Maccioni, and G. Costantini, "Toward the design of a wearable system for fall-risk detection in telerehabilitation," *Telemed. E-Health,* vol. 15, no. 3, pp. 296-299, 2009.